# 운동학적 제약조건을 이용한 심해저 라이저의 비선형 동적해석

# Nonlinear Dynamic Analysis of Deep Water Riser by the Utilization of the Kinematic Constraint Condition

홍 남 식*
Hong, Nam-Seeg

요 지

변형된 라이저의 단위 접선벡터상의 운동학적 제약조건을 적용하여 심해저 라이저의 비선형 동적해석을 행한다. 이 조건의 적용으로 자유도수를 감소시킬수 있으며 심한 비선형성으로 인한 해의 발산 가능성을 제거할 수 있다. 라이저의 거대변형으로 인한 기하학적 비선형성과 비선형 경계조건이 고려된다. 또한, 비선형성이 포함되는 수동학적 하중이 조류와 파랑에 의해 발생하여 내부에 정상류가 흐르는 라이저관의 외벽에 작용하게 된다. 이외에도 라이저 자체의 축방향 변형조건을 고려한다. Galerkin의 유한요소 근사화와 시간증분자를 적용하여 유한요소에 대한 평형 메트릭스 방정식을 유도하고, 수치해석을 위한 알고리즘을 제안하며 API 보고서의 결과와 비교함으로써 제안된 모델이 검증된다. 또한, 기하학적 비선형성으로 인한 영향을 조사하였다.

**핵심용어** : 운동학적 제약조건, 심해저 라이저, 기하학적 비선형성

Abstract

The kinematic constraint condition on unit tangent vector of deflected riser is utilized in the nonlinear dynamic analysis of deep water riser. This does lead to the reduction of the degrees of freedom and remove the possibility of the divergence in solutions. The riser system accounts for the geometric nonlinearity due to large structural displacements and the nonlinear boundary conditions. And also, it includes a steady flow inside the pipe which is modeled as an extensible or inextensible, tubular beam subject to nonlinear hydrodynamic loads such as current or wave excitation. The matrix equation of equilibrium for the finite element system is constructed by applying Galerkin finite element approximation and the time incremental operator and then, the algorithm for numerical calculation is proposed. The validity of proposed model is given through the comparison with the results from API reports. Also, the effect of geometrical nonlinearity is examined.

***Keyword*** : *Kinematic constraint condition, Deep water riser, Geometric nonlinearity*

## 1. Introduction

In offshore operation, as the water depth becomes deeper, the displacements of a riser (Fig. 1) will become larger. Therefore, it is desirable to consider the nonlinearities due to

* 정회원 · 동아대학교 토목해양공학부, 전임강사

· 이 논문에 대한 토론을 1999년 12월 31일까지 본 학회에 보내주시면 2000년 3월호에 그 결과를 게재하겠습니다.

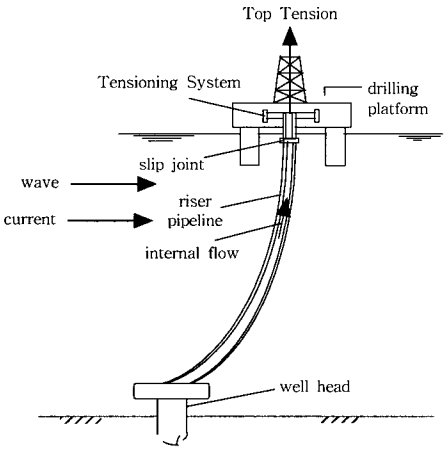


Fig. 1 Configuration of riser system

large displacements for the riser analysis. The nonlinearities are mainly of two origin that results from flow-induced forces and from geometric nonlinearities due to large structural deflections. The later becomes particularly significant for long risers. Such nonlinearities are from large deflections and slopes, three-dimensional bending, extensibility, torsion, dependency of the hydrodynamic loads on the riser deformation and nonlinear boundary conditions.

There are considerable efforts made over the years to this problem. The equations for large amplitude three dimensional inextensible motions of beams were derived by Nordgren[1], with the assumption of constant principal moments of inertia, negligible rotatory inertia, and the uncoupled torsional motion. Bruce and Michael[2] described a mathematical model and solution technique for a system with coupled dynamic axial and lateral responses of a riser column. Fellipa and Chung[3] implemented a finite element method for solving nonlinear static equilibrium configurations of deep water risers. Also, a transient analysis was developed by Chung[4] for the determination of nonlinear motion by considering nonlinear static configuration as an initial condition. Garett[5] presented a three dimensional finite element model of an inextensible elastic rod with equal principal stiffness. The model permitted large deflections and finite rotations and accounted for tensional variation along its length. Konuk[6] provided a general foundation for developing rigorous formulation of problems involving marine pipelines with twist. Safai[7] developed a method for automatically updating the structural geometry during the dynamic analysis for a system in which the bending, axial and torsional vibrations are uncoupled. Kim and Triantafyllou[8] studied the nonlinear dynamics of long, slender cylinders assuming moderately large deformations and no longitudinal excitation modes. McNamara and Lane[9] presented an efficient method based on the finite element approach using convected coordinates for arbitrary large rotations. Huang and Chucheepsakul[10] introduced a method of static analysis for risers with a relative slippage at the location of the slip joint. The method introduced a modified functional involving multipliers to account for the arc length being unvaried with neglected tension, and used the exact curvature of radius in their formulation. Bernitsas and Kokarakis[11] formulated the problem of static three dimensional nonlinear, large deformation response of a riser within small strain theory and then solved it numerically by using an incremental finite element algorithm, in which predictor-corrector scheme is involved. Later, they (Kokarakis and Bernitsas)[12] employed a previously formulated static model for the dynamic analysis of riser and developed an efficient algorithm. O'Brien and McNamara[13] developed a technique based on finite element method by the separation of the rigid body motions from deformations of element

under the condition of finite rotations. Hong[14),15)] proposed a mathematical model with the inclusion of internal flow and the aforementioned nonlinear effects and then solve it numerically by using Newton Raphson iterative procedure.

Most of aforementioned papers use the arc length as the independent variable to formulate the problem. In analysis the use of the arc length as the independent variable may cause complexity in setting up problem. This complexity may lead to the necessity for a large number of iterations to obtain a single solution numerically. These iterations are divided into two groups. The first one involves the solution of a set of nonlinear algebraic equations associated with the geometric nonlinearity. The second group of iterations arises from the boundary condition. The problem may be solved by estimating a riser length measured from the well head, then finding the horizontal displacement at the elevation of the top joint by either the finite element method or finite difference method. If the horizontal displacement does not correspond to the location of the joint, estimate again the riser length and repeat the process until the error at the boundary is negligible. The estimations of the riser length constitute the second group of iterations. It is apparent that each iteration in the second group requires a number of iterations of the first group.

The purpose of this study is to propose a method of analysis in which the complexity mentioned above is completely eliminated. The kinematic constraint condition on unit tangent vector of deflected riser is utilized. This does lead to the reduction of the degrees of freedom and remove the possibility of the divergence in solution due to the iteration of highly nonlinear terms.

In the analysis presented herein only two dimensional cases are considered, although the methodology developed can be readily extended to three dimensional cases. The riser system accounts for the nonlinear effects due to large structural displacements and from the nonlinear boundary conditions, and includes a steady flow inside the pipe which is modeled as an extensible or inextensible, tubular beam subject to nonlinear hydrodynamic loads such as current or wave excitation. The matrix equation of equilibrium for the finite element system is constructed by applying Galerkin finite element approximation and the time incremental operator and then, the algorithm for numerical calculation is proposed. The validity of proposed model is given through the comparison with the results from API reports. Also, the effect of geometrical nonlinearity is examined.

## 2. Governing Equations AND B.C.s

The main aspects of the curved geometry of the system and the coordinate systems are depicted in Fig. 2. In Fig. 2, "~" indicates a unit vector and hereafter boldface represents general vectors. The total bending moment, as shown in Fig. 2, acts in the binomial direction and is proportional to the bending rigidity of the cross section EI, and the space curve will be identified with the central axis of the riser in the deformed state, with the position vector, as shown in Fig. 2, represented as follows.

$$\mathbf{r} = \mathbf{r}_0 + s\hat{k} = x_1\hat{i} + x_2\hat{j} + (s + x_3)\hat{k} \qquad (1)$$

where $\mathbf{r}_0$ is the deformation vector at any point on the riser in the undeformed state.

In the classical theory of rods, the internal state of stress at a point on the rod is

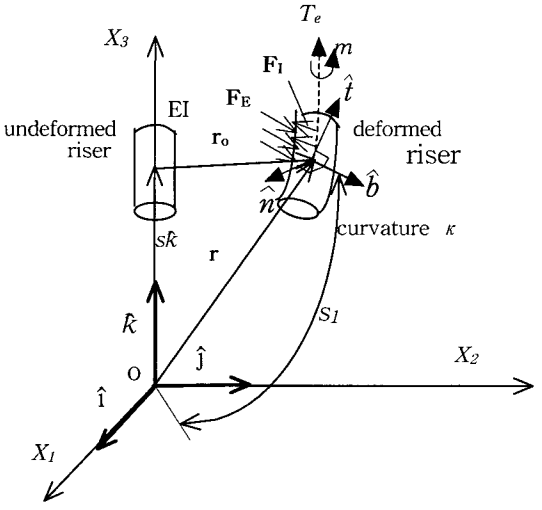


Fig. 2 Position vector at a point on the riser centerline

fully characterized by the resultant force **F** and the coupled moment **M** acting on the central axis. Assuming that the distributed coupled vector induced by the asymmetric flow and rotatory inertia is negligible and that the torsional couple H is independent of pipe length, conservation of linear momentum and angular momentum leads to the following vector equation of motion.

$$-(EI\mathbf{r}'')'' + [(T_e - EI\kappa^2)\mathbf{r}']' + H(\mathbf{r}' \times \mathbf{r}'')' + \mathbf{F}_E + \mathbf{F}_I = m_r \ddot{\mathbf{r}} \quad (2)$$

where $\mathbf{F}_E$, $\mathbf{F}_I$ and $m_r$ are the applied external hydrodynamic force, the force acting inside the wall of riser by internally flowing fluid, and the mass of riser per unit length, respectively. Also, EI is the bending rigidity of the cross section and H is the time dependent torque. Prime(′) and dot( · ) denotes differentiation with respect to undeformed arc length s and time, respectively. The effective tension $T_e$, which is the tangential component of the internal force, is defined by

$$T_e = \hat{t} \cdot \mathbf{F} \quad (3)$$

Using the concept of Hamilton's principle, Hong[14] derived the fluid force acting on the internal wall of the pipe by internally flowing fluid and expressed in the following vector form.

$$\mathbf{F}_I = -m_f(\ddot{\mathbf{r}} + 2V_I \dot{\mathbf{r}}' + V_I^2 \mathbf{r}'') \quad (4)$$

where $V_I$ and $m_f$ are the velocity of internal flow and the mass of internal flowing fluid per unit riser length.

No small-scale motions such as turbulence or secondary flow are assumed to be absent. And also, the plug-flow model with no radial variation of velocity is utilized as a fluid model for the internal flow. The first term on the right represents the inertia force associated with the riser acceleration. The second term is the inertia force associated with the coriolis acceleration which arise because the fluid is flowing with velocity $V_I$ relative to the riser, while the riser itself has an angular velocity at any point along its length. The last term represents the inertia force associated with the change in direction of the flow velocity, owing to the curvature of the riser.

The relative motion between the pipe and the surrounding fluid produces hydrodynamic force composed of inertia, drag, and frictional forces. The resultant total force distribution $\mathbf{F}_E$ along the riser length is decomposed of a normal force component, $\mathbf{F}_N$, and a tangential component, $\mathbf{F}_T$. To perform this decomposition, the relative velocity and acceleration is resolved into components perpendicular and parallel to the deformed riser axis. The relative velocity vector between the pipe and the surrounding fluid is given by

$$\mathbf{V}_R = \mathbf{V}_P - \mathbf{V}_C - \mathbf{V}_W = \dot{\mathbf{r}} - \mathbf{V}_C - \mathbf{V}_W \qquad (5)$$

where $\mathbf{V}_P$ = pipe velocity vector, $\mathbf{V}_C$ = steady current velocity vector, and $\mathbf{V}_W$ = time dependent wave velocity vector. Noting that the current velocity is independent of time, the relative acceleration of the pipe with respect to the surrounding fluid is given by

$$\dot{\mathbf{V}}_R = \dot{\mathbf{V}}_P - \dot{\mathbf{V}}_W = \ddot{\mathbf{r}} - \dot{\mathbf{V}}_W \qquad (6)$$

and its tangential and normal components are given by

$$\dot{\mathbf{V}}_{RT} = (\dot{\mathbf{V}}_R \cdot \hat{t})\hat{t} \quad \text{and} \quad \dot{\mathbf{V}}_{RN} = \dot{\mathbf{V}}_R - \dot{\mathbf{V}}_{RT} \qquad (7)$$

Also we need the tangential and normal components of wave-induced water particle acceleration to calculate wave induced force and they are given by

$$\dot{\mathbf{V}}_{WT} = (\dot{\mathbf{V}}_W \cdot \hat{t})\hat{t} \quad \text{and} \quad \dot{\mathbf{V}}_{WN} = \dot{\mathbf{V}}_W - \dot{\mathbf{V}}_{WT} \qquad (8)$$

Chung[4] neglected the tangential force comnent by skin friction and then, retained only the normal force component as shown in following form.

$$\mathbf{F}_E \approx \mathbf{F}_N = -\rho_w(\pi D_o^2/4)C_A \dot{\mathbf{V}}_{RN} + \rho_w(\pi D_o^2/4) \dot{\mathbf{V}}_{WN} - \rho_w D_o C_D |\mathbf{V}_{RN}| \mathbf{V}_{RN}/2 \qquad (9)$$

where $|\mathbf{V}_{RN}| = [\,V^2_{RN1} + V^2_{RN2} + V^2_{RN3}\,]^{1/2}$, $C_A$ = added mass coefficient, $C_D$ = drag coefficient, $D_o$ = external diameter of the pipe, and $\rho_w$ = density of water.

The first term of Eq. (9) is an inertia term representing the force that is required to accelerate the pipe with respect to the surrounding water. The second term is the wave induced force. This force is produced by the local pressure gradient that accompanies the normal component of water particle acceleration. The last term is the drag force that is proportional to the square of the normal velocity component and formed by the separation of flow.

Substituting Eqs. (4) and (9) into Eq. (2),

$$m_r \ddot{\mathbf{r}} + (EI\mathbf{r}'')'' - [(T_e - EI\kappa^2)\mathbf{r}']' - H(\mathbf{r}' \times \mathbf{r}'')' = -m_f(\ddot{\mathbf{r}} + 2V_I \dot{\mathbf{r}}' + V_I^2 \mathbf{r}'') - \rho_w(\pi D_o^2/4)C_A \dot{\mathbf{V}}_{RN} + \rho_w(\pi D_o^2/4) \dot{\mathbf{V}}_{WN} - \rho_w D_O C_D |\mathbf{V}_{RN}| \mathbf{V}_{RN}/2 \qquad (10)$$

Letting $A_O = \pi D_O^2/4$, $m_t = m_r + m_f + \rho_w A_O C_A$,

$$\boldsymbol{q} = -\frac{1}{2}\rho_w C_D D_O |\mathbf{V}_{RN}| \mathbf{V}_{RN} + \rho_w A_O(1+C_A) \dot{\mathbf{V}}_W + \rho_w A_O C_A(\hat{t} \cdot \ddot{\mathbf{r}})\hat{t} - \rho_w A_O(1+C_A)(\hat{t} \cdot \dot{\mathbf{V}}_W)\hat{t} \qquad (11)$$

and then manipulating, we have nonlinear governing vector equation shown as

$$m_t \ddot{\mathbf{r}} + 2m_f V_I \dot{\mathbf{r}}' + m_f V_I^2 \mathbf{r}'' + (EI\mathbf{r}'')'' - [(T_e - EI\kappa^2)\boldsymbol{r}']' - H(\boldsymbol{r}' \times \boldsymbol{r}'')' = \boldsymbol{q} \qquad (12)$$

For the completion of the mathematical model, the boundary conditions have to be specified. The boundary conditions for the dynamic model of riser are usually time dependent because of the motions of the supporting platform. The riser support can be modeled by substituting the linear translational or rotational springs providing the restoring boundary forces and moments. Typically the displacement or the force vector and the unit tangent vector, or the bending or torsional moment has to be specified at each riser end. From

the equilibrium of the forces at the top yields:

$$F_{1u}=(TF)\hat{t}\cdot\hat{i}-K_1x_{1u}$$
$$F_{2u}=(TF)\hat{t}\cdot\hat{j}-K_2x_{2u}$$
$$F_{3u}=(TF)\hat{t}\cdot\hat{k}-K_3x_{3u}+TTR \qquad (13)$$

In eq.(13), the subscript $u$ and i(i=1,2,3) indicates the upper end of the riser and $X_i$ direction respectively. TTR is the tension applied at top of the riser by the tensioning system and $K_1$, $K_2$, $K_3$ are spring constants supplied by the restoring boundary force. Also the effective riser tension at the top of riser may be given approximately.

$$TF\approx\rho_w g\pi D_o^2(S_w-z)/4-\rho_m g\pi D_i^2(S_m-z)/4 \quad (14)$$

where $S_w$ = ordinate of the free surface of water, $S_m$ = ordinate of the free surface of mud, $\rho_w$ and $\rho_m$ are the density of water and mud respectively, $D_o$ and $D_i$ are external and internal diameter of the riser and z is measured. from the lower ball joint, i.e., z = s + $x_3$.

## 3. Matrix Dynamic Equilibrium Equation

The numerical model of governing equations and boundary conditions is developed using finite element method. Variational statement for the boundary value problem is introduced, that is, the weak form of governing equation is derived. Sequentially, the incremental operator is applied to the weak form to give the following equation(Hong[4),5)] ; Bernitsas and Kokarakis[11)]).

$$\int_0^{l_{1i}} m_t\,\Delta\dot{\mathbf{r}}\cdot\bar{\mathbf{r}}\,ds_1+\int_0^{l_{1i}}2m_f V_I\,\Delta\dot{\mathbf{r}}'\cdot\bar{\mathbf{r}}\,ds_1$$
$$-\int_0^{l_{1i}} m_f V_I^2\Delta\mathbf{r}'\cdot\bar{\mathbf{r}}'\,ds_1+\int_0^{l_{1i}}(EI\,\Delta\mathbf{r}'')\cdot\bar{\mathbf{r}}''\,ds_1$$
$$-\int_0^{l_{1i}}(T_e-EIx^2)\Delta\mathbf{r}'\cdot\bar{\mathbf{r}}\,ds_1+\int_0^{l_{1i}}(\mathbf{F}\cdot\Delta\mathbf{r}')(\mathbf{r}'\cdot\bar{\mathbf{r}}')ds_1$$
$$-\int_0^{l_{1i}}(2EI\mathbf{r}''\cdot\Delta\mathbf{r}'')(\mathbf{r}'\cdot\bar{\mathbf{r}}')ds_1+\int_0^{l_{1i}}H(\Delta\mathbf{r}'\times\mathbf{r}'')\cdot\mathbf{r}'ds_1$$
$$+\int_0^{l_{1i}}H(\mathbf{r}'\times\mathbf{r}'')\cdot\bar{\mathbf{r}}'ds_1$$
$$=\{-m_f V_I^2\Delta\mathbf{r}'+\Delta\mathbf{F}\}\cdot\bar{\mathbf{r}}\mid_0^{l_{1i}}+EI\Delta\mathbf{r}''\cdot\bar{\mathbf{r}}\mid_0^{l_{1i}}$$
$$+\int_0^{l_{1i}}\Delta\mathbf{q}\cdot\bar{\mathbf{r}}ds_1-\int_0^{l_{1i}}(\Delta\mathbf{F}\cdot\mathbf{r}')(\mathbf{r}'\cdot\bar{\mathbf{r}})ds_1 \qquad (15)$$

where $l_{1i}=\int_0^{l_i}(1+\varepsilon_t)ds$ , $l_i$ = the length of i−th element

This is the incremental weak form of the governing equation and the quantities in front of integrals are considered constants for each element so that those terms may be factored out of the integrals.

The construction of a finite element approximation of the problem, such as given in (15), is based on Galerkin's decomposition method. Here, we replace (15) by a finite dimensional problem to find the approximate solution vector $\mathbf{r}_h$. The nodal values of the approximate solution are unknown functions of time and consists of not only the deflections at the nodes, but also the rotations. In other words, after constructing interpolation functions on a suitable mesh, we take the approximate solution to be of the form

$$\mathbf{r}_h=x_{1h}\hat{i}+x_{2h}\hat{j}+(x_{3h}+s)\hat{k} \quad \text{and}$$
$$x_{jh}(s_1,t)=\sum_{i=1}^{4}x_{ji}(t)N_i(s_1), \quad j=1,2,3 \qquad (16)$$

where $x_{j1},x_{j3}$ and $x_{j2},x_{j4}$ represent the deflections and the rotations at node, and $N_i$ is the basis or interpolation function. Having selected the basis functions, the incremental form of an approximate solution and the test function can be written similarly

$$\triangle x_{jh}(s_1, t) = \sum_{i=1}^{4} \triangle x_{ji}(t) N_i(s_1),$$

$$x_{jh}(s_1, t) = \sum_{i=1}^{4} x_{ji}(t) N_i(s_1) \tag{17}$$

The substitution of (16), (17) into (15) introduces the series form of the incremental weak form. Manipulationg the series form and writing them in a matrix form. we obtain the following matrix equilibrium equation :

$$[M]\{\triangle \ddot{x}\} + [C]\{\dot{x}\} + [K]\{\triangle x\} = \{\triangle f\} + \{\triangle F\} \tag{18}$$

## 4. Utilization of Kinematic Constraint Condition

The utilization of the kinematic constraint on unit tangent vector makes it feasible to represent the vertical degrees of freedom in terms of the lateral ones. This does lead to the reduction of the degrees of freedom per element from 12 to 8 and remove the possibility of the divergence in solutions due to the iteration of highly nonlinear terms in the vertical degrees of freedom. Moreover, it can be implemented as an another algorithm scheme for the iteration due to nonlinear terms. For the development of an algorithm, the derivation of the incremental form of the extensibility condition is necessary because the equations of equilibrium for a finite element system in motion to be solved is of the incremental form.

Using the kinematic constraint on unit tangent vector of riser, i.e. $\hat{t} \cdot \hat{t} = \mathbf{r}' \cdot \mathbf{r}' = 1$, we have the following relationship :

$$x_1'^2 + x_2'^2 + (x_3' + 1/(1+\varepsilon_t))^2 = 1 \tag{19}$$

Applying the incremental operator $\triangle$ on above equation. We obtain

$$\triangle x_3' = -(x_1' \triangle x_1' + x_2' \triangle x_2')(x_3' + 1/(1+\varepsilon_t))^{-1} + \triangle \varepsilon_t (1+\varepsilon_t)^{-2} \tag{20}$$

also, we have

$$T_e = \mathbf{F} \cdot \hat{t} = \mathbf{F} \cdot \mathbf{r}' = F_1 x_1' + F_2 x_2' + F_3 (x_3' + 1/(1+\varepsilon_t)) \tag{21}$$

Applying the incremental operator on Eq. (21). We get

$$\triangle T_e = \triangle F_1 x_1' + \triangle F_2 x_2' + \triangle F_3 (x_3' + 1/(+\varepsilon_t)) + F_1 \triangle x_1' + F_2 \triangle x_2' + F_3 \triangle x_3' - F_3 \triangle \varepsilon_t (1+\varepsilon_t)^{-2} \tag{22}$$

Also, we have

$$T_e = EA\varepsilon_t + \rho_w A_o g(S_w - S - x_3) - \rho_w A_i g(S_m - S - x_3) \tag{23}$$

Applying $\triangle$ again on Eq. (23). we obtain

$$\triangle T_e = EA \triangle \varepsilon_t - \triangle x_3 g(\rho_w A_0 - \rho_m A_i) \tag{24}$$

Eliminating $\triangle$Te from Eqs. (22) and (24), we compute $\triangle \varepsilon_t$

$$\triangle \varepsilon_t = \{\triangle F_1 x_1' + \triangle F_2 x_2' + \triangle F_3 (x_3' + 1/(1+\varepsilon_t)) + F_1 \triangle x_1' + F_2 \triangle x_2' + F_3 \triangle x_3' + \triangle x_3 g(\rho_w A_o - \rho_m A_i)\} / \{EA + F_3 (1+\varepsilon_t)^{-2}\} \tag{25}$$

Substituting Eq. (25) into Eq. (20) and solving for $\triangle x_3'$, we obtain

$$\triangle x_3' = \left(1 + \frac{F_3}{EA(1+\varepsilon_t)^2}\right)\left[-\frac{x_1 \triangle x_1' + x_2 \triangle x_2'}{x_3' + 1/(1+\varepsilon_t)} + \frac{1}{EA(1+\varepsilon_t)^2 + F_3}\{\triangle F_1 x_1' + \triangle F_2 x_2'\right.$$

$$\triangle F_3(x_3' + 1/(1+\varepsilon_t)) + \triangle F_1 x_1' + \triangle F_2 x_2' + \triangle x_3 g(\rho_w A_o - \rho_m A_i)\}] \quad (26)$$

In addition to Eq. (26). we also have

$$\triangle x_3 = \int_0^{s_1} \triangle x_3' \, ds_1$$

$$x_3' = (1 - x_1'^2 - x_2'^2)^{1/2} - 1/(1+\varepsilon_t)$$

$$x_3 = x_3(0) + \int_0^{s_1} x_3' \, ds_1 \quad (27)$$

As stated earlier, the vertical degrees of freedom can be computed in terms of the lateral ones. For each load increment the kinematic relations, Eqs. (26) and (27), are used to remove the vertical degrees of freedom from global matrix equation of equilibrium. They are used again after the solution of the reduced system of equations has been achieved. During prediction phase, $x_3, x_3', \triangle x_3, \triangle x_3'$ are computed using Eqs. (26) and (27). In addition, during the prediction phase equation (18) are used to compute $x_1, x_1', \triangle x_2, \triangle x_2', \triangle x_2, \triangle x_2'$. During the correction phase $x_3, x_3', \triangle x_3, \triangle x_3'$ are recomputed using Eqs. (26)-(27) and all deformation dependent matrices, the equivalent nodal forces, the boundary conditions, and the lengths of elements are corrected. Further $x_1, x_1', \triangle x_1, x_2, x_2', \triangle x_2, \triangle x_2'$ are recomputed using Eq.(18). This scheme is repeated until convergence is achieved for each load increment. The algorithm is summarized in Fig. 3.

## 5. Numerical Application

The algorithm described in the previous chapter is implemented to solve the incremental form of the matrix equilibrium equation and to avoid the possibility of divergence due to iterations and to improve convertgence rate, and computer program is written. For the purpose of investigating the validity of the suggested model in this paper, Results of analysis using the riser program are compared to the published results from eight other programs in API[16]. A two dimensional model is adopted as in the API report, and Morison's formula extended for a moving structure based on the relative velocity between the riser section and the fluid is employed to approximate the fluid drag force. The investigated example is concerned with the same type of riser with an external diameter of 40.64cm (16 in), the water depth of 152.40m, and top tension of 53.4 dN. A wave of 6.096 m of amplitude and a period of 9 sec is applied and the prescribed horizontal displacement at the head of the riser varies sinusoidally with the same period as the wave. As for the tension at the head, it is assumed to be constant during the dynamic calculation. In Fig. 4, envelopes of minimum and maximum horizontal displacements by the present method are compared with the results published in API and show good overall agreement.

Also, the comparison of the results obtained from well-known linear model with one from the developed nonlinear model is given. It is well known from previous studies that the nonlinear effects due to large structural deflections and nonlinear drag damping become significant as riser length increases or internal tension decreases. On the contrary, the nonlinear effects disappear for the riser with high tension and short length. In this paper, linear model and nonlinear model are both run using the same riser with parameters listed in Table 1, and then compared with each other to see the difference between linear model and nonlinear model due to the change of riser length. The flow field is generated by a linear wave ($H_w$= 6.1m, $T_w$=7.8sec) and a uniform current (U=0.4 m/sec) with an right angle to each other.

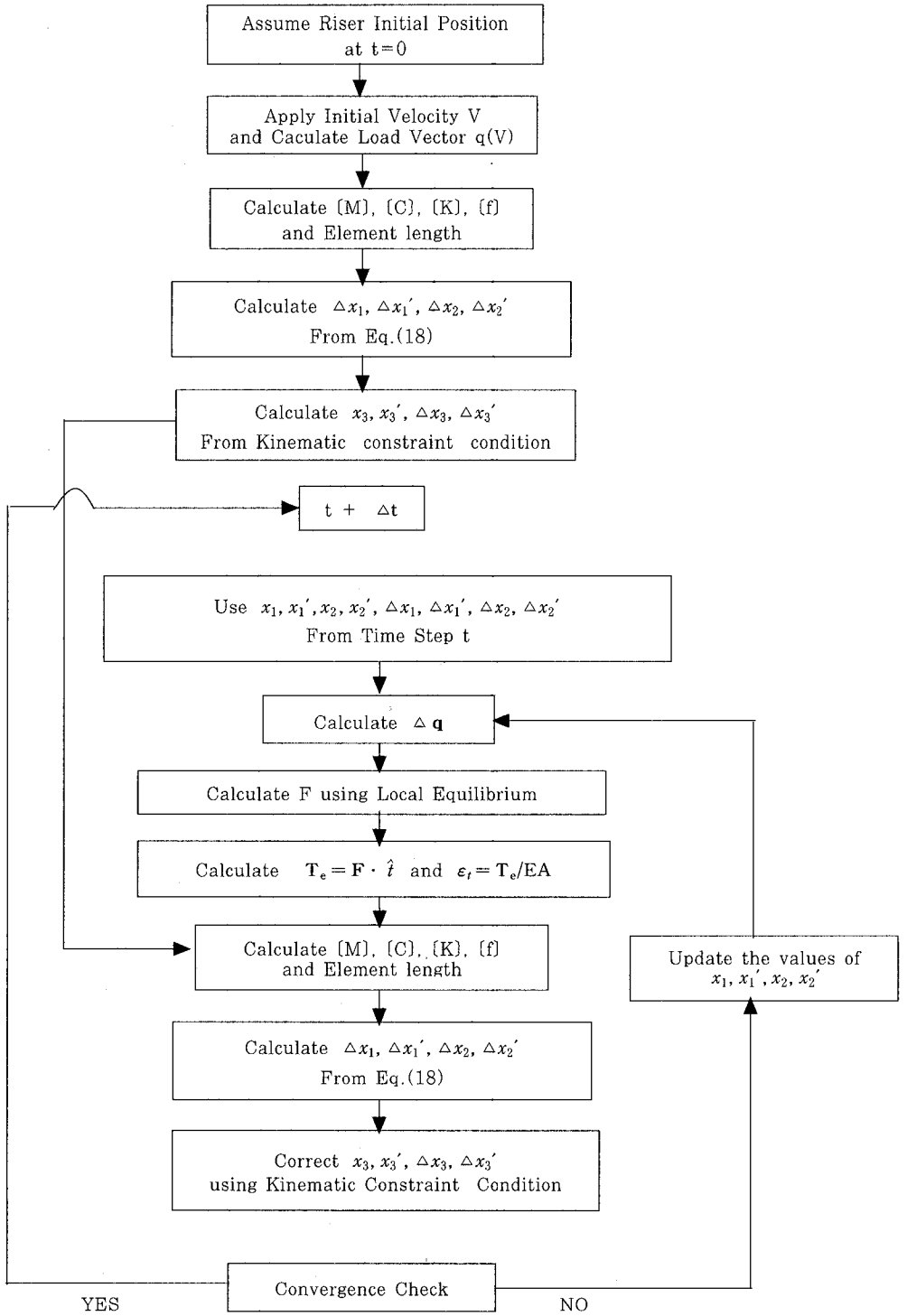


Fig. 3 Solution algorithm

Fig. 5 plot time simulations of displace- ment at the middle of the riser in current direction, respectively. Two different length of risers, one long(152m) and the other one short(91m), are used with same top and bottom tensions. From those figure, the reduction of nonlinear effect on the short one can be seen. Also, from those time simulation plots, the nonlinear effect in the long riser causes change of the system frequency. The displacement shapes at a specific time are presented in Fig. 6 and 7 for current and

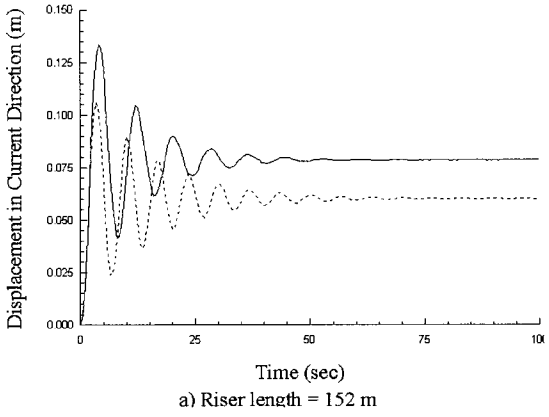


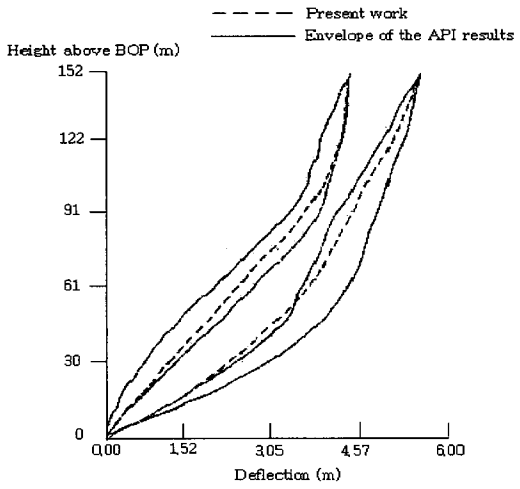


Fig. 4 Comparison with API cases

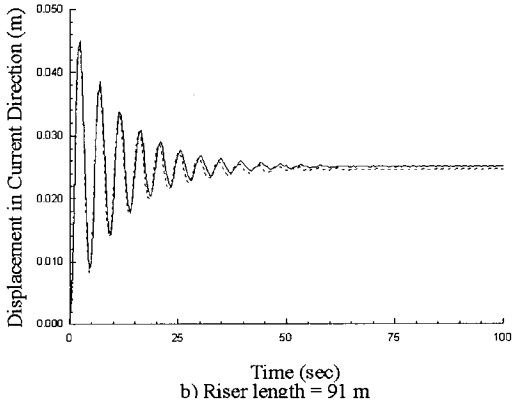


Fig. 5 Time simulations of the displacement at the middle of riser in current direction. (Dashed Line = Nonlinear Model, Solid Line = Linear Model)

Table 1 Design properties and data for a drilling riser system

| | |
|---|---|
| Outside diameter | D = 0.61 m with 16 mm wall thickness |
| Constant of elasticity | E = 2.1 x $10^6$ kg/$cm^2$ |
| Sectional moment of inertia | I = 131018 $cm^4$ |
| Riser mass | m = 10 kg/cm(include mass of drilling mud and sea water) |
| Bottom tension | TTB = 1200 kN |
| Effective weight per unit length | w = 3.86 kN/m |
| Mean Tension | $\overline{T_e}$= 1453 kN |
| Density of drilling mud | $\rho$m = 1.36 t/$m^3$ |
| Density of sea water | $\rho$w = 1.036 t/$m^3$ |

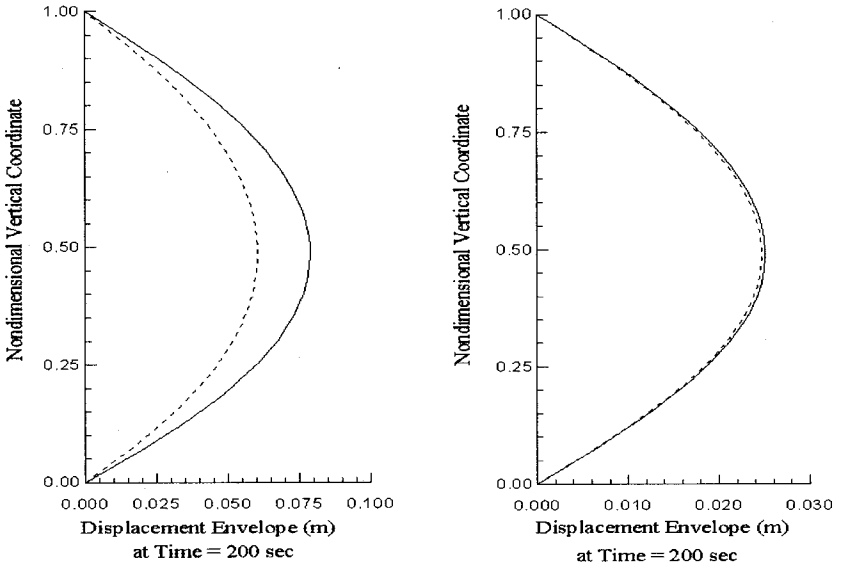


(a) Riser length = 152 m (b) Riser length = 91 m

Fig. 6 Displacement envelope in current direction.(Dashed Line = Nonlinear Model, Solid Line = Linear Model)

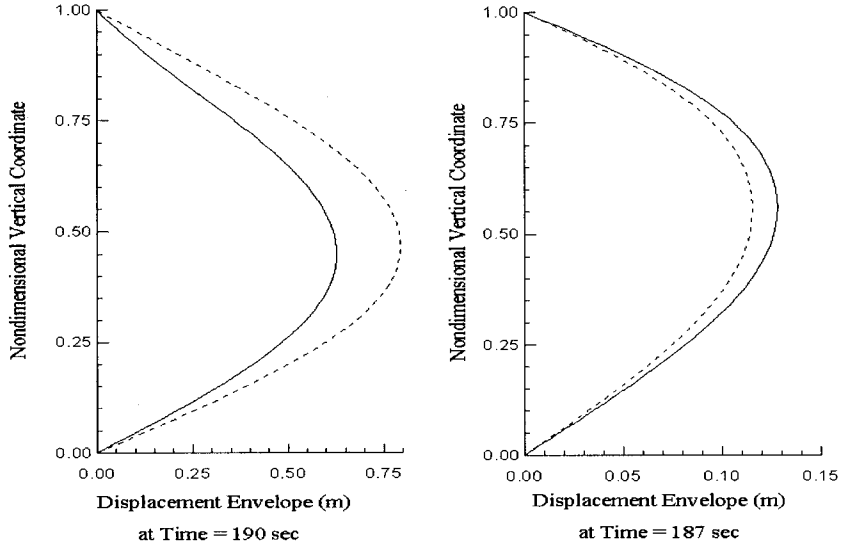


(a) Riser length = 152 m (b) Riser length = 91 m

Fig. 7 Displacement envelope in wave direction. (Dashed Line = Nonlinear Model, Solid Line = Linear Model)

wave direction, respectively. The displacement shape in current direction are plotted at time=200sec after the riser reaches the static state, while the shapes in wave direction are plotted at an arbitrary time when the displacement at the middle point of riser is near the positive peak. The difference between linear and nonlinear models grows as riser length increases. The nonlinear effect appears to stiffen the riser for current loading but soften it for wave loading. These trends are also found from previous study(Kokarakis and Bernitsas12)). Fig. 8 shows the maximum displacement in the wave direction according to the change of wave frequency. The responsein the wave direction also shows resonant peaks near the system frequencies but the magnitudes are drastically reduced for higher frequency wave. This phenomenon seems to result from the fact that the wave velocity distribution in water depth decays faster for shorter frequency waves.

Trajectory of displacement at the middle of riser is presented in Fig. 9. In this figure, the riser responds to current at a right angle to wave direction after a steady oscillating state in wave direction has been reached and the top tension ratio(TR=Top Tension/wL) is changed from 2.6 to 1.2 for the reduction of stiffness term. Since a high velocity of current (U=1.5m/sec) and a reduced top tension (TR=1.2) are selected, it can be seen clearly from the figure that the oscillation of riser in current direction reaches a static state within 2 to 3 cycles with the longer period. In addition, it can be recognized from the figure that the time trajectory shape is transformed into more regular shape because of a wave with relatively low period (Tw=4sec) in this application. This trend of time trajectory can be also found in Mcnamara's study[13].

## 6. Conclusion

In order to eliminate the complexity in the nonlinear dynamic analysis of riser, the kinematic constraint condition on unit tangent vector of deflected riser is utilized. This does lead to the reduction of the degrees of freedom and remove the possibility of the divergence in solution due to the iteration of highly nonlinear terms.

The riser system accounts for the nonlinear effects due to large structural displace-

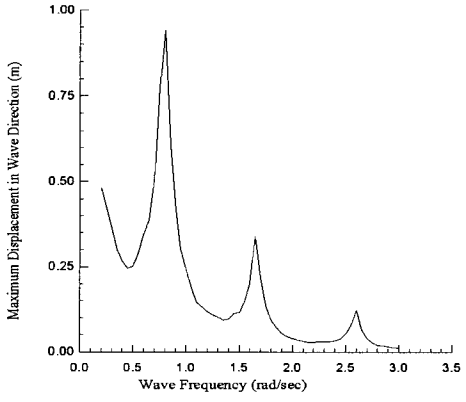


Fig. 8 Maximum displacement in wave direction according to the change of wave Frequency(Hw=6.1m)

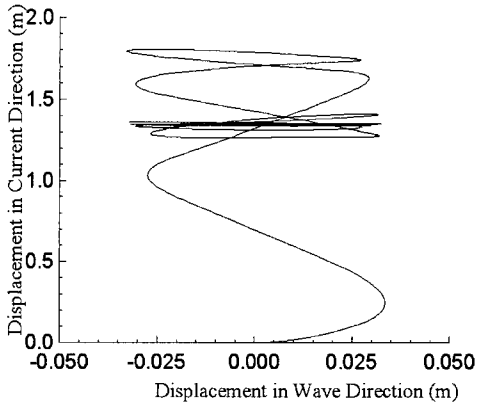


Fig. 9 Time trajectory at the middle of a 152m riser(Hw=6.1m).

ments and from the nonlinear boundary conditions, and includes a steady flow inside the pipe which is modeled as an extensible or inextensible, tubular beam subject to nonlinear hydrodynamic loads such as current or wave excitation. The incremental matrix equation of equilibrium is constructed and the algorithm for numerical calculation is proposed.

From the results of sample computations, it is found that the effect of geometric nonlinearity becomes increasingly more important for risers in deeper water and that the linear model underestimates the displacement as compared to nonlinear model.

## Acknowledgements

This study has been undertaken as a part of research sponsored by Science and Research Foundation of Kangnung National University. Contact period : 1998.5.1.-1999.4.30.

## Rererences

1. Nordgren, R.P., "On Computation of the Motion of Elastic Rods", *ASME Journal of Applied Mechanics*, Vol. 96, Sep.1974, pp.777~780
2. Bruce, E.B. and Michael, F.M., Nonlinear Dynamic Analysis of Coupled Axial and Lateral Motion of Marine Risers, *Offshore Technology Conference*, OTC 2776, Houston, Texas, 1977, pp.403~412
3. Fellipa, C.A. and Chung, J.S., "Nonlinear Static Analysis of Deep Ocean Mining Pipe - Part I: Modeling and Formulation", *ASME Journal of Energy Resources Technology*, Vol.103, Mar.1981, pp.11~15
4. Chung, J.S., "Nonlinear Transient Motion of Deep Ocean Mining Pipe", *ASME Journal of Energy Resources Technology*, Vol.103, Mar.1981, pp.2~10
5. Garrett, D.L., "Dynamic Analysis of Slender Rods", *ASME Journal of Energy Resources Technology*, Vol.104, Dec.1982, pp.302~306
6. Konuk, I., "Application of an Adaptive Numerical Technique 3-D Pipeline Problems with Strong Nonlinearities", *ASME Journal of Energy Resources Technology*, Vol.104, Mar.1982, pp.58~62
7. Safai, V.M., "Nonlinear Dynamic Analysis of Deep Water Risers", *Applied Ocean Research*, Vol.5, No.4, 1983, pp.215~225
8. Kim, Y.C. and Triantafyllou, M.S., "The Nonlinear Dynamics of Long, Slender Cylinders", *ASME Journal of Energy Resources Technology*, Vol.106, June 1984, pp.250~256
9. McNamara, J.F. and Lane, M., "Practical Modeling for Articulated Risers and Loading Columns", *ASME Journal of Energy Resources Technology*, Vol.106, Dec.1984, pp.444~450
10. Huang, T. and Chucheepsakul, S., "Large Displacement Analysis of a Marine Riser", *ASME Journal of Energy Resources Technology*, Vol.107, Mar.1985, pp.54~59
11. Bernitsas, M.M. and Kokarakis, J.E., "Large Deformation Three-Dimensional Static Analysis of Deep Water Marine Risers", *Applied Ocean Research*, Vol.7, No.4, 1985, pp.178~187
12. Kokarakis, J.E. and Bernitsas, M.M., "Nonlinear Three Dimensional Dynamic Analysis of Marine Risers", *ASME Journal of Energy Resources Technology*, Vol.109, Sep.1987, pp.105~111
13. O'Brien, P.J. and McNamara, J.F., "Three Dimensional Nonlinear Motions of Risers and Offshore Loading Towers", *ASME Journal of Offshore Mechanics and Arctic Engineering*, Vol.110, 1988, pp.232~237

14. Hong, N.S., "The Effect of Internal Flow on Marine Riser Dynamics", Ph.D. Dissertation, University of Florida at Gainesville, USA, 1994, pp.171
15. Hong, N.S., "The Effect of Internal Flow on Marine Riser Dynamics", *KSCOE Journal of Coastal and Ocean Engineering*, Vol. 7, No. 1, pp. 75-90, 1995
16. American Petroleum Institute, "Comparison of Marine Drilling Riser Analysis", API Bulletin 2J, 1st edition, Jan. 1977

(접수일자 : 1999. 5. 26)